JACS
JOURNAL OF THE AMERICAN CHEMICAL SOCIETY
Article
pubs.acs.org/JACS

Pd-Catalyzed Electrohydrogenation of Carbon Dioxide to Formate: High Mass Activity at Low Overpotential and Identification of the Deactivation Pathway

Xiaoquan Min and Matthew W. Kanan*

Department of Chemistry, Stanford University, Stanford, California 94305, United States

Supporting Information

ABSTRACT: Electrochemical reduction of CO_2 to formate (HCO_2^-) powered by renewable electricity is a possible carbon-negative alternative to synthesizing formate from fossil fuels. This process is energetically inefficient because >1 V of overpotential is required for CO_2 reduction to HCO_2^- on the metals currently used as cathodic catalysts. Pd reduces CO_2 to HCO_2^- with no overpotential, but this activity has previously been limited to low synthesis rates and plagued by an unidentified deactivation pathway. Here we show that Pd nanoparticles dispersed on a carbon support reach high mass activities (50−80 mA HCO_2^- synthesis per mg Pd) when driven by less than 200 mV of overpotential in aqueous bicarbonate solutions. Electrokinetic measurements are consistent with a mechanism in which the rate-determining step is the addition of electrochemically generated surface adsorbed hydrogen to CO_2 (i.e., electrohydrogenation). The electrodes deactivate over the course of several hours because of a minor pathway that forms CO. Activity is recovered, however, by removing CO with brief air exposure.

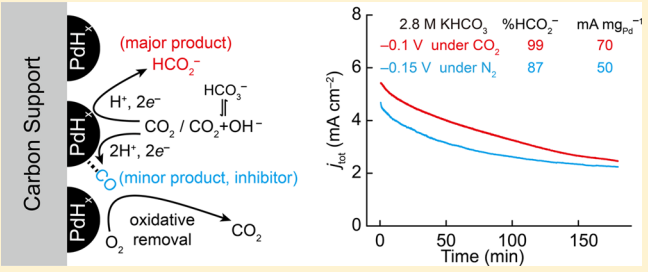

INTRODUCTION

Converting CO_2 and H_2O into commodity chemicals using renewable energy could significantly reduce CO_2 emissions by replacing existing fossil fuel−based syntheses.[1−3] Formic acid (HCO_2H) and formate salts (M^+ HCO_2^-) are relatively high-value commodity chemicals that are currently synthesized from CO that is produced by steam reforming natural gas. A possible replacement for this route is to convert CO_2 into HCO_2^- by hydrogenation or electrochemical reduction in the presence of a base. While several effective CO_2 hydrogenation catalysts have been developed,[4−8] this approach requires a separate step that produces H_2 using renewable energy in order to synthesize HCO_2^- with a net consumption of CO_2. Moreover, most hydrogenation catalysts need high H_2 pressures (>40 bar) to achieve acceptable rates. Electrochemical reduction of CO_2 to HCO_2^- (eq 1) could be powered directly by renewable electricity and avoids handling H_2.[9] The main challenge for this approach is to reduce CO_2 at high rates with a minimum amount of overpotential in order to minimize the energy requirement.[10−12] The equilibrium potential for the CO_2/HCO_2^- couple at pH 7 is approximately 0 V vs the reversible hydrogen electrode (RHE; all potentials are given with respect to this reference).[13] Early studies showed that p-block metals including Sn and Pb selectively reduce CO_2 to HCO_2^- in aqueous solutions at potentials ≤−1 V (≥1 V of absolute overpotential).[14−18] More recently, researchers have developed nanostructured electrodes,[19] composite materials,[20] molecular electrocatalysts,[12,21,22] and N-doped carbon electrode materials[23] that reduce CO_2 to HCO_2^- in water. These studies have opened new avenues of research, but the overpotentials required (>0.8 V) are still too large for practical use.

$$CO_2 + 2e^- + HCO_3^- \rightarrow HCO_2^- + CO_3^{2-} \quad (1)$$

Pd is typically considered to be an inefficient CO_2 electroreduction catalyst that produces CO as the major carbon-containing product. Studies of Pd foil electrodes in CO_2-saturated aqueous HCO_3^- solution reported 5 mA cm^{-2} current density with 10−30% Faraday efficiency (FE) for CO and 0−3% FE for HCO_2^- at −0.8 to −1.0 V.[15−18] The rest of the current under these conditions corresponds to H_2 evolution and hydrogen absorption into the Pd lattice. In contrast with these results, two earlier studies unmasked an alternative pathway in which Pd selectively reduces CO_2 to HCO_2^- at minimal overpotential but only at low current densities. An electrode comprised of Pd nanoparticles imbedded in a conductive polymer produced HCO_2^- with up to 85% FE and a maximum geometric current density of 100 μA cm^{-2} at 0 V in HCO_3^- solution.[13] Attempts to increase the current density by applying overpotential resulted in exclusive H^+ reduction. An electrochemically deposited Pd electrode with a much higher Pd loading produced HCO_2^- with 95% FE and a maximum current density of 300 μA cm^{-2} at 0 V.[24] A recent study of Pd−Pt electrodes demonstrated HCO_2^- formation at

Received: November 22, 2014
Published: March 26, 2015

DOI: 10.1021/ja511890h
J. Am. Chem. Soc. 2015, 137, 4701−4708

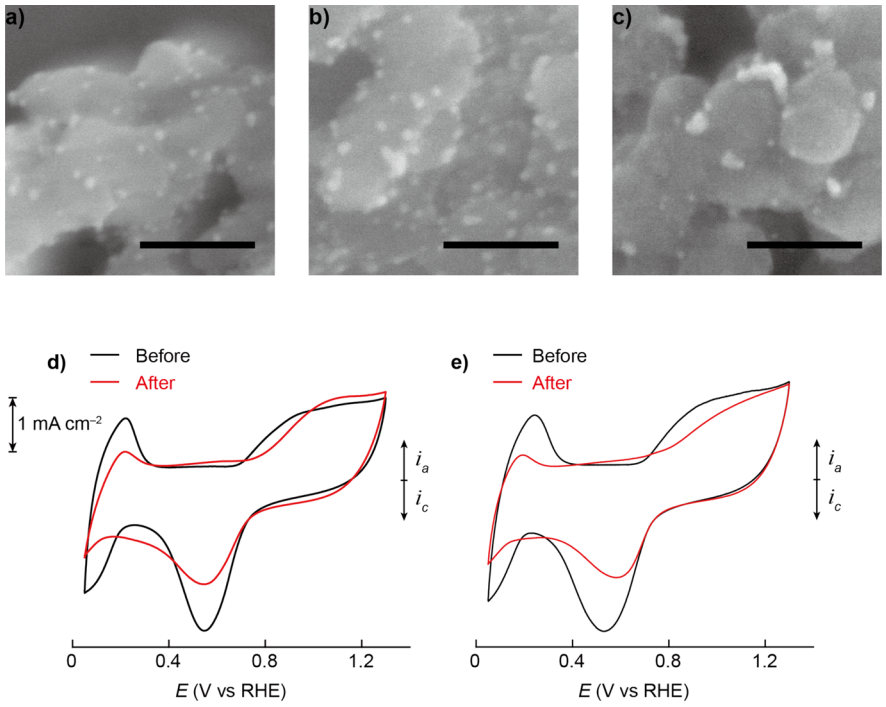

Figure 1. SEM characterization and electrochemical surface area (ECSA) measurements of Pd/C electrodes before and after electrolysis in CO_2-saturated 0.5 M $NaHCO_3$. SEM images: (a) before; (b) after 3 h at −0.25 V vs RHE; (c) after 3 h at −0.35 V. All scale bars are 50 nm. ECSA measurements before and after 3 h of electrolysis: (d) at −0.25 V; (e) at −0.35 V. Cyclic voltammetry was performed in 0.5 M H_2SO_4 with a scan rate of 50 mV/s.

potentials close to 0 V, although the efficiency was not determined.[25]

Despite the attraction of reducing CO_2 at minimal overpotential, Pd has not been pursued as a catalyst for electrochemical HCO_2^- synthesis. Because of its cost, the use of Pd would require electrodes with high mass activities, high current densities, and long lifetimes. The maximum current densities for HCO_2^- synthesis achieved with the nanoparticle and electrodeposited Pd electrodes described above are far below the CO_2 mass transport limits for solution phase electrolyses. The inability to achieve higher HCO_2^- synthesis rates with larger overpotentials on these electrodes, combined with the radically different product distribution at high overpotential on Pd foil, suggest that Pd loses the ability to reduce CO_2 to HCO_2^- beyond a narrow potential range around 0 V. One subsequent study of Pd in gas diffusion electrodes, which provide much higher concentrations of CO_2 at the catalyst surface, reported 70% FE for HCO_2^- and 18 mA cm^{-2} geometric current density with an unspecified mass loading, but only for electrolyses lasting 4 min.[26] Determining what is necessary to drive CO_2 reduction to HCO_2^- at high rates on Pd and elucidating the cause(s) of deactivation could open the possibility of using this material for scalable electrochemical HCO_2^- synthesis with unprecedented energetic efficiency.

Here we show that CO_2 reduction to HCO_2^- proceeds at high mass activity and high current density on Pd nanoparticle electrodes when driven by small overpotentials and that deactivation of this catalysis is caused by CO poisoning. With less than 200 mV of overpotential, Pd on carbon (Pd/C) electrodes reduce CO_2 to HCO_2^- at up to 80 mA per mg Pd averaged over 3 h in both CO_2-saturated and N_2-saturated HCO_3^- solutions. CO is formed as a minor product at a potential-dependent rate and binds tightly to the Pd surface to inhibit electrocatalytic activity at low overpotential. Brief exposure to air removes CO to restore activity. Our results provide a foundation for developing practical Pd-based catalysts for energetically efficient electrochemical HCO_2^- synthesis.

RESULTS

To determine whether Pd is capable of reducing CO_2 to HCO_2^- with high mass activity, we evaluated the catalytic activity of 10 wt% Pd on C (Pd/C). Scanning electron microscopy (SEM) indicated that this material is composed of Pd nanoparticles with ∼5 nm diameters dispersed on ∼100 nm carbon particles (Figure 1a). Electrodes were prepared by depositing 0.5 mg cm^{-2} of the Pd/C onto Ti substrates, which corresponds to a Pd loading of 50 μg cm^{-2} (see Supporting Information (SI) and Figure S2). The electrocatalytic activity and electrokinetics of CO_2 reduction were evaluated by performing constant-potential electrolyses in CO_2- or N_2-saturated aqueous HCO_3^- solutions at ambient temperature. The saturating gas was continuously sparged through the catholyte at 5 mL min^{-1} and fed into the sample loop of a gas chromatograph to quantify the gas-phase products at 15−20 min intervals. HCO_2^- was quantified by NMR analysis at the end of the electrolyses (Figure S9). Independently prepared electrodes evaluated under identical conditions exhibited variability of <15% for the current density and <5 percentage points for the Faradaic efficiencies.

The activity of Pd/C was first assessed in CO_2-saturated 0.5 M $NaHCO_3$ (pH 7.2) at selected potentials between −0.05 and −0.35 V (ca. 50−350 mV of overpotential for HCO_2^- production). The total geometric current density (j_{tot}) at the beginning of the electrolyses ranged from 0.9 mA cm^{-2} at −0.05 V to 6.5 mA cm^{-2} at −0.35 V (Figure 2a). In all cases, j_{tot} declined as the electrolysis proceeded. The rate of decline was slow at −0.05 V, but it increased as the potential was made

DOI: 10.1021/ja511890h
J. Am. Chem. Soc. 2015, 137, 4701−4708

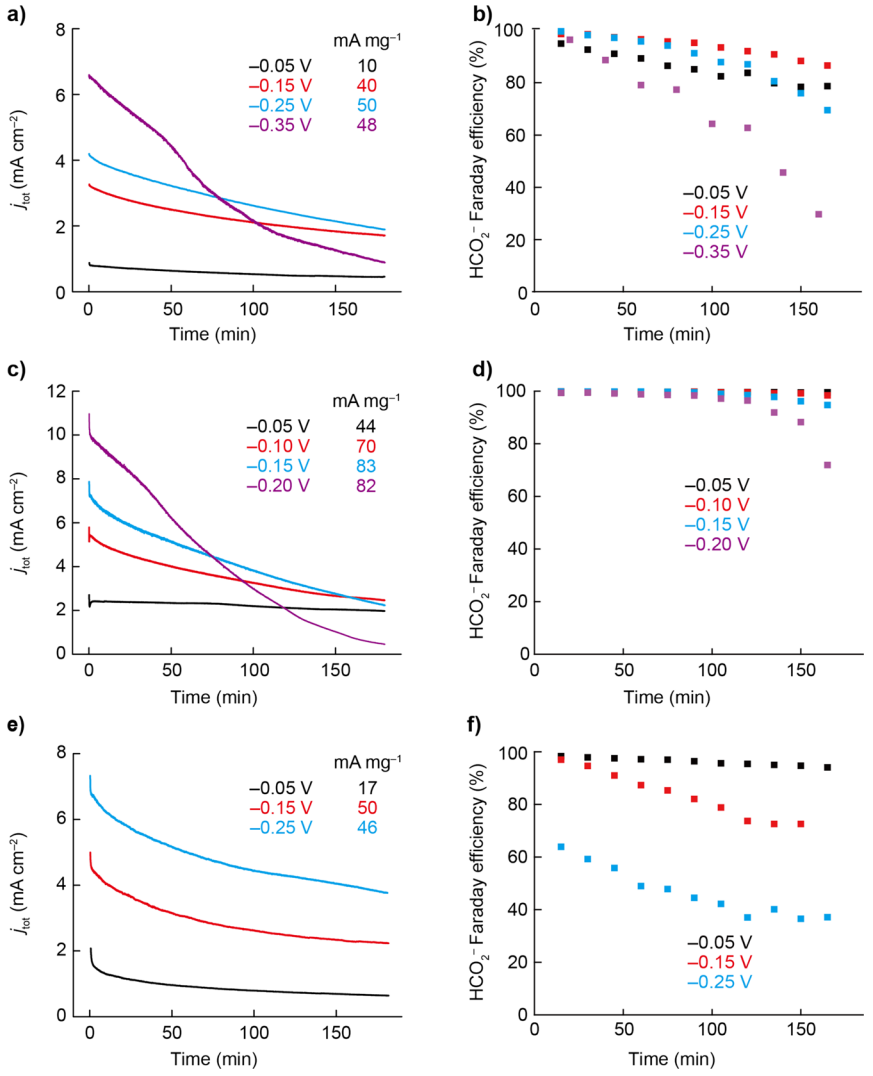

Figure 2. CO_2 reduction activity of Pd/C electrodes in three different electrolytes. (a,c,e) Total geometric current density (j_{tot}) vs time and the mass activity for HCO_2^- synthesis averaged over 3 h. (b,d,f) HCO_2^- Faraday efficiency vs time. Electrolyses were performed in CO_2-saturated 0.5 M $NaHCO_3$ (a,b); CO_2-saturated 2.8 M $KHCO_3$ (c,d); and N_2-saturated 2.8 M $KHCO_3$ (e,f). The mass activities were determined by quantifying the HCO_2^- at the end of the electrolyses using NMR. The HCO_2^- Faraday efficiencies vs time were calculated by subtracting the H_2 Faraday efficiency (determined by periodic GC analysis) from the total efficiency.

more cathodic. At −0.25 V, ∼45% of the initial j_{tot} was lost over 3 h, while at −0.35 V, ∼85% was lost. At −0.05 to −0.25 V, the average FE for HCO_2^- over 3 h was 86−94% and H_2 was the only other detectable product. The average mass activity (mA HCO_2^- production per mg Pd) over 3 h was 10 mA mg^{-1} at −0.05 V and increased to 50 mA mg^{-1} at −0.25 V (Table S1). The corresponding partial current densities for HCO_2^- synthesis ($j_{formate}$) were 0.5 mA cm^{-2} and 2.5 mA cm^{-2}. The FE for HCO_2^- slowly decreased over the course of each electrolysis (Figure 2b). For the electrolysis at −0.35 V, the average FE for HCO_2^- during the first 2 h was 88%, corresponding to an average mass activity of 69 mA mg^{-1} and an average $j_{formate}$ of 3.45 mA cm^{-2}. Trace amounts of CO were detected as j_{tot} decreased to <40% of its initial value (Figure S3).

Electrolysis under identical conditions with Pd foil electrodes produced no HCO_2^- after 12 h at −0.05 or −0.25 V (Figure S7). Over the time scale of several hours, hydrogen absorption accounts for essentially all of the current on Pd foil because of its low surface area to mass ratio (see Discussion). Ti foil itself and carbon powder were also incapable of CO_2 reduction to HCO_2^-, producing ≪1% of the current density observed for the Pd/C electrodes (see SI and Figure S2).

To determine if the activity could be improved at higher [HCO_3^-], a second set of electrolyses was performed in CO_2-saturated 2.8 M $KHCO_3$ solution. ($KHCO_3$ has higher solubility compared to $NaHCO_3$). Significantly higher rates and FE for HCO_2^- synthesis were obtained in this electrolyte compared to CO_2-saturated 0.5 M $NaHCO_3$ (Figure 2c,d). At −0.05 to −0.15 V, the initial j_{tot} values were 2.4 to 7 mA cm^{-2}, which corresponded to initial mass activities of 48 to 140 mA mg^{-1}. The FE was nearly quantitative for the first hour and still ≥95% after 3 h. The activities declined at a potential dependent rate, with 20% lost over 3 h at −0.05 V and 70% lost over 3 h at −0.15 V. When averaged over the entire 3 h of electrolysis, mass activities at −0.05 to −0.15 V were 44 to 83 mA mg^{-1}, corresponding to $j_{formate}$ values of 2.2 to 4.15 mA cm^{-2}. At −0.2 V, the activity declined precipitously after ∼50 min of electrolysis. Prior to this decline, however, $j_{formate}$ was 10 mA cm^{-2} and the mass activity reached 188 mA mg^{-1}.

DOI: 10.1021/ja511890h
J. Am. Chem. Soc. 2015, 137, 4701−4708

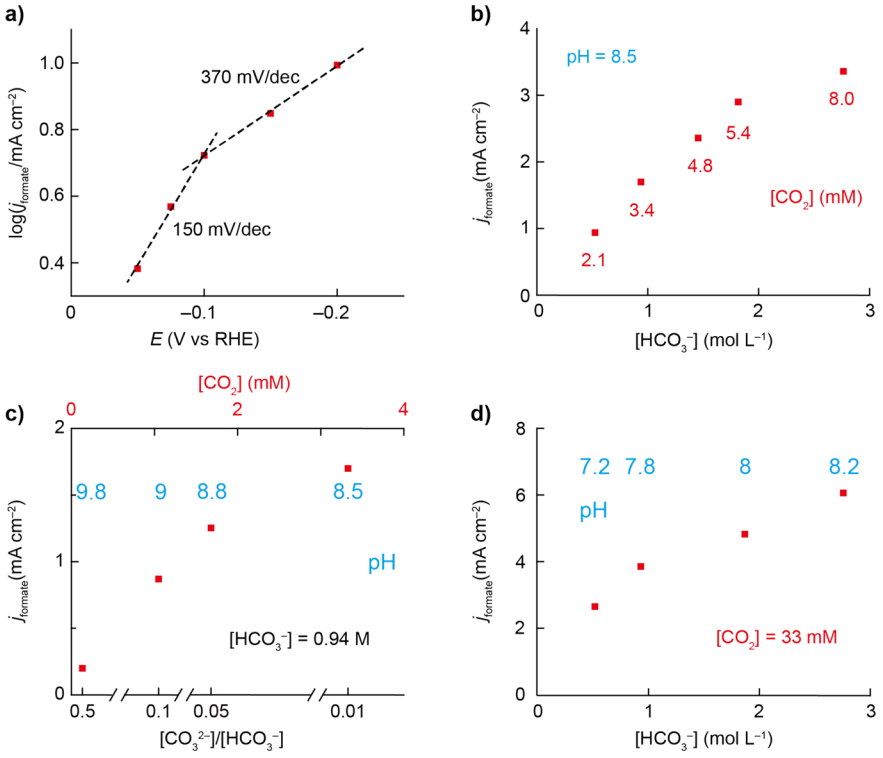

Figure 3. Electrokinetics of CO_2 reduction to HCO_2^- on Pd/C electrodes. $j_{formate}$ is the partial current density for HCO_2^- production. (a) Tafel plot ($\log(j_{formate})$ vs E) in CO_2-saturated 2.8 M $KHCO_3$. (b) $j_{formate}$ vs $[HCO_3^-]$ in N_2-saturated $KHCO_3$ at −0.15 V. (c) $j_{formate}$ vs $[CO_3^{2-}]/[HCO_3^-]$ in N_2-saturated 0.94 M $KHCO_3$ at −0.15 V. (d) $j_{formate}$ vs $[HCO_3^-]$ in CO_2-saturated $KHCO_3$ at −0.15 V. $j_{formate}$ values were averaged over 5 min of bulk electrolysis in (a), and averaged over 1 h of bulk electrolysis in (b,c,d). The pH values of the solutions (blue) were measured. The corresponding $[CO_2]$ values (red) were calculated from eqs 2 and 3.

To see if high mass activities could be achieved in the absence of gaseous CO_2, a series of electrolyses were performed with Pd/C electrodes in N_2-saturated 2.8 M $KHCO_3$. Although it was lower than in CO_2-saturated 2.8 M $KHCO_3$, the activity for HCO_2^- synthesis was still substantial in the N_2-saturated electrolyte. The FE for HCO_2^- was >95% over 3 h at −0.05 V, while larger amounts of H_2 were produced at more negative potentials. The mass activities averaged over 3 h were 17, 48, 44 mA mg^{-1} at −0.05, −0.15, −0.25 V, respectively. The relatively high activity for HCO_2^- synthesis in N_2-saturated HCO_3^- arises from reduction of CO_2 that is in equilibrium with HCO_3^- (see below).

To probe the mechanism of CO_2 reduction with Pd/C, the electrokinetic parameters were measured by performing additional constant-potential electrolyses. The electrochemical equation (eq 1) indicates that the rate could depend on the potential, $[CO_2]$, $[HCO_3^-]$, and pH. The potential dependence was measured while holding the other three variables constant by performing electrolyses in CO_2-saturated 2.8 M $KHCO_3$. The Tafel plot ($\log(j_{formate})$ vs potential) exhibited an approximate slope of 150 mV dec^{-1} from −0.05 to −0.1 V and 370 mV dec^{-1} at larger overpotentials (Figure 3a). The 150 mV dec^{-1} slope is similar to values that were previously measured for an electrochemically deposited Pd electrode at potentials close to 0 vs RHE.[24] As discussed below, this value is consistent with an electrohydrogenation mechanism with a rate-limiting chemical reaction involving adsorbed hydrogen, assuming a Temkin isotherm for the surface hydrogen coverage (θ_H).[24] The 370 mV dec^{-1} slope at larger overpotentials, where $j_{formate}$ becomes nearly independent of potential, is likely the result of saturation of θ_H, as well as possibly CO poisoning and mass transport limitations.

The $[CO_2]$, $[HCO_3^-]$, and pH cannot be varied independently because they are related by the following equilibria (eq 2 and eq 3):

$$CO_2 + H_2O \leftrightarrows HCO_3^- + H^+ \quad pK_{a1} = 6.35\ (25°C) \tag{2}$$

$$HCO_3^- \leftrightarrows CO_3^{2-} + H^+ \quad pK_{a2} = 10.33\ (25°C) \tag{3}$$

To determine the dependences on these variables, $j_{formate}$ was measured at a constant potential of −0.15 V vs RHE over a series of experiments in which the concentration(s) of the carbon species were varied. First, electrolyses were performed in N_2-saturated $KHCO_3$ electrolyte with different HCO_3^- concentrations. Under N_2 saturation with freshly prepared electrolytes, the pH is 8.5 over a wide range of $[HCO_3^-]$, but $[CO_2]$ increases in proportion to $[HCO_3^-]$ because of the equilibrium in eq 2. As seen in Figure 3b, $j_{formate}$ increased linearly as $[HCO_3^-]$ was increased from 0.5 to 1.8 M, which corresponds to increasing $[CO_2]$ from 2.1 to 5.4 mM (Figure 3b). (To calculate $[CO_2]$, activity coefficients were taken from Roy et al., see SI for more details)[27] This result demonstrates that $j_{formate}$ has an approximately first-order dependence on either HCO_3^- or CO_2. The fact that $j_{formate}$ approaches a limiting value of 10 mA cm^{-2} at large overpotential (Figure 3a) indicates that the reduction substrate is most likely CO_2 instead of HCO_3^-, and therefore the reaction is first-order in CO_2. Much higher limiting current densities would be expected if HCO_3^- were the substrate because it is present in high concentration.

DOI: 10.1021/ja511890h
J. Am. Chem. Soc. 2015, 137, 4701−4708

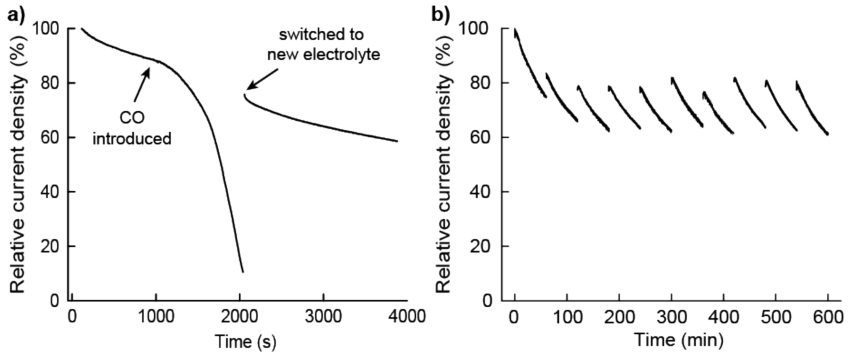

Figure 4. CO poisoning and recovery of activity with Pd/C. (a) Relative current density vs time for an electrolysis at −0.25 V in CO_2-saturated 0.5 M $NaHCO_3$ with CO added at a rate of 0.5 mL min^{-1} as beginning at t = 900 s. At t = 2000 s, the electrode was exposed to air and transferred to a new CO-free electrolyte, and electrolysis was restarted at −0.25 V. (b) Relative current density vs time for a series of 1 h electrolyses at −0.25 V in CO_2-saturated 0.5 M $NaHCO_3$ with a single Pd/C electrode. The electrode was exposed to air and transferred to a fresh electrolyte each time. The average Faraday efficiency for HCO_2^- was 95% in the first electrolysis and 90% in each of the subsequent electrolyses.

Next, electrolyses were performed under N_2 with $[KHCO_3]$ held constant at 0.94 M and different amounts of K_2CO_3 added to the electrolyte to change $[CO_2]$ and pH. (Increasing $[CO_3^{2-}]$ at constant $[HCO_3^-]$ decreases $[CO_2]$ and increases the pH.) As the $[CO_3^{2-}]/[HCO_3^-]$ ratio was changed from 0.01 to 0.5, which decreases $[CO_2]$ from 3.4 to 0.13 mM, $j_{formate}$ decreased from 1.7 to 0.2 mA cm^{-2} (Figure 3c). This result provides further support for substrate being CO_2 instead of HCO_3^-. However, the dependence on $[CO_2]$ is weaker in Figure 3c compared to Figure 3b. Since the pH is also changing in Figure 3c, this result suggests that increasing the pH at constant potential vs RHE has a positive effect on $j_{formate}$, which mitigates the decrease in $j_{formate}$ that results from decreasing $[CO_2]$. To further test the effect of pH, electrolyses were performed in CO_2-saturated $KHCO_3$ electrolyte with different concentrations of HCO_3^-. Under CO_2 saturation, $[CO_2]$ is fixed at 33 mM, but the pH increases as $[HCO_3^-]$ is increased. As the pH was increased from 7.2 to 8.2 by adding HCO_3^-, $j_{formate}$ increased from 2.6 to 6 mA cm^{-2} (Figure 3d), which is consistent with the pH effect deduced from the data in Figure 3c. This effect likely arises from a pH dependence of θ_H at constant potential vs RHE (see Discussion).

The activity of Pd/C shown in Figures 2 and 3 significantly exceeds all other known materials under comparable conditions (see Discussion). This catalysis is limited, however, by a deactivation process that occurs at a potential-dependent rate. To determine the cause(s) of deactivation, we first assessed whether electrolysis caused morphological changes to the Pd nanoparticles. Electrodes were analyzed by SEM after 3 h of electrolysis at −0.25 or −0.35 V in CO_2-saturated 0.5 M $NaHCO_3$. A small increase in the average size of the Pd nanoparticles was evident after electrolysis at −0.25 V, (Figure1b) while significantly larger Pd aggregates were observed after electrolysis at −0.35 V (Figure1c). The changes in Pd surface area were estimated by comparing the size of the surface oxide reduction wave in cyclic voltammagrams obtained before and after electrolysis (Figure 1d, e).[28] The Pd electrochemical surface area (ECSA) measured for an unused 2 cm^2 Pd/C electrode was approximately 50 cm^2 (corresponding to a roughness factor of 25). The ECSA was reduced by 30 and 50% after 3 h of electrolysis at −0.25 and −0.35 V, respectively. These results demonstrate that the Pd nanoparticles sinter on the carbon support under CO_2 reduction conditions. However, the reduction in surface area does not account for all of the loss of HCO_2^- production activity during electrolysis with Pd/C electrodes, which implicates a second cause of deactivation.

Because trace CO was observed after most of the activity was lost at −0.35 V (Figure S3), we hypothesized that CO is formed as a minor product of CO_2 reduction and inhibits HCO_2^- formation as it accumulates on the Pd nanoparticle surfaces. CO_2 reduction has been proposed to be the source of CO poisoning on Pd electrodes used as catalysts for HCO_2H electrooxidation.[29,30] CO poisoning was also implicated in the deactivation of the recently reported Pd−Pt catalyst for CO_2 reduction.[25] To test whether the formation of CO deactivates CO_2 reduction to HCO_2^- on Pd nanoparticles, we first determined whether CO is an inhibitor by deliberately adding it to the electrolyte. Electrolysis was started with a fresh Pd/C electrode at −0.25 V in CO_2-saturated 0.5 M $NaHCO_3$ as described above. After 15 min, a flow of CO was added to the electrolyte at a rate of 0.5 mL min^{-1}. j_{tot} declined to <10% of its initial value within 20 min of the start of CO addition (Figure 4a), indicating that CO is a potent inhibitor of all electroreduction activity at this potential. CO is typically removed from Pd surfaces by oxidation.[31,32] At ambient temperature, O_2 adsorbs dissociatively on Pd surfaces[33,34] and the adsorbed oxygen reacts with CO to form CO_2.[35] To see if air oxidation is sufficient to remove CO and restore CO_2 reduction activity, the electrode was briefly exposed to air and transferred to a new CO_2-saturated HCO_3^- electrolyte. Upon restarting electrolysis at −0.25 V, j_{tot} recovered to 75% of its initial value and the FE for HCO_2^- was >95%.

If CO formation deactivates CO_2 reduction on Pd/C, the results above indicate that exposing the electrode to air will restore activity. To test for this recovery, we performed a series of 1 h electrolyses in CO_2-saturated 0.5 M $NaHCO_3$ electrolyte at −0.25 V with a single Pd/C electrode (Figure 4b). After each electrolysis, the electrode was briefly exposed to air and transferred to a fresh electrolyte before starting the subsequent electrolysis. The use of a fresh electrolyte ensured that CO did not accumulate in the cell over the course of the experiment. During the first electrolysis, j_{tot} declined by 30% from its initial value. Exposure to air resulted in partial recovery of j_{tot}. Thereafter, each exposure to air completely restored the j_{tot} lost in the preceding electrolysis. The average FE for HCO_2^- was 95% in the first electrolysis and ∼90% for each of the remaining electrolyses. Thus, exposure to air repeatedly restored activity for CO_2 reduction to HCO_2^-. The activity loss in the first electrolysis that was not recovered likely reflects the loss of

DOI: 10.1021/ja511890h
J. Am. Chem. Soc. 2015, 137, 4701−4708

surface area due to nanoparticle sintering (see above). Activity lost during electrolysis in N_2-saturated 2.8 M $KHCO_3$ was similarly recovered by air exposure (Figure S5), demonstrating that CO poisoning causes deactivation under these conditions as well.

To assess the stability of Pd/C electrodes in the absence of CO formation, electrolyses were performed at −0.25 V in N_2-saturated Na_2CO_3 solution. Unlike HCO_3^-, there is no significant rate of CO_2 formation from CO_3^{2-}, which precludes CO_2 reduction and the formation of CO in this electrolyte. As expected, H_2 was the only observed reduction product. j_{tot} declined by only 35% over the first 8 h of electrolysis and then stabilized (Figure S6). In contrast, j_{tot} declined by 90% over 8 h of electrolysis in CO_2-saturated $NaHCO_3$ without air exposure to remove CO. The 35% loss of activity for Pd/C in Na_2CO_3 electrolyte is consistent with loss of surface area due to sintering that occurs regardless of which reduction reaction takes place.

DISCUSSION

Electrochemical reduction of CO_2 to HCO_2^- near the equilibrium potential is exclusive to Pd and the enzyme formate dehydrogenase.[36,37] Our results show that modest overpotentials drive this reaction to high rates with dispersed Pd nanoparticles on a carbon support. With a Pd mass loading of only 50 μg cm^{-2}, Pd/C electrodes reach geometric current densities as high as 10 mA cm^{-2} of HCO_2^- synthesis at −0.2 V vs RHE, corresponding to specific (Pd surface area-normalized) current density of 400 μA cm^{-2}. Under comparable conditions, other catalysts require at least 700 mV of additional overpotential to reach similar activity. This large disparity most likely reflects a fundamental difference in the mechanism of CO_2 reduction to HCO_2^-. On most materials, the reaction requires electron transfer to CO_2, which imposes a large overpotential. On Pd, the data presented here and in previous studies[13,24] support an electrohydrogenation mechanism in which CO_2 is converted to HCO_2^- by electrochemically generated PdH.

Pd nanoparticles catalyze chemical hydrogenation of HCO_3^-/CO_2 to HCO_2^- at ambient temperature with 1 atm H_2, which is the equivalent of 0 vs RHE.[38] In these studies, Pd/C attained initial hydrogenation turnover frequencies as high as 20 nmol of HCO_2^- synthesized per cm^2 of Pd per h, which is the equivalent of a specific current density of 1 μA cm^{-2} for electrochemical HCO_2^- synthesis. On an electrode, when Pd is held at potentials <0 V vs RHE, its equilibrium state is a β-phase PdH (PdHx where $x \sim 0.7$).[39] The surface hydride on this material should reduce CO_2 in the same way as surface hydride generated by reaction of Pd nanoparticles with H_2. Under electrochemical conditions, the reaction is accelerated relative to chemical hydrogenation with 1 atm H_2 by applying overpotential to increase θ_H (see below). Since the Pd nanoparticles in Pd/C have a high surface area-to-mass ratio, the transition from Pd into β-PdH requires only tens of seconds and CO_2 reduction to HCO_2^- becomes the dominant process thereafter. For Pd foil, the surface area-to-mass ratio is approximately 0.02 cm^2 mg^{-1} and H absorption to generate PdH requires many hours. As a result, no significant HCO_2^- production is seen for Pd foil in this time period.

The electrokinetic measurements in Figure 3 support a rate law given by eq 4:

$$j = k[CO_2]\exp(-\alpha EF/RT) \quad (4)$$

where k is a potential-independent rate constant and α is the transfer coefficient and E is the potential vs RHE. At potentials ranging from −0.05 to −0.1 V vs RHE, α is approximately 0.4, which corresponds to a Tafel slope of 150 mV dec^{-1}. As described previously by Podlovchenko et al., a Tafel slope near 118 mV dec^{-1} (α = 0.5) is consistent with a mechanism that involves rate-limiting addition of electrochemically adsorbed hydrogen to the substrate.[24] Such a mechanism for CO_2 reduction with Pd nanoparticles is shown in Scheme 1.

Scheme 1. Electrohydrogenation Mechanism for CO_2 Reduction on Pd/C

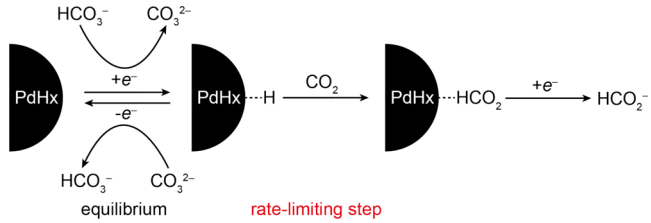

Reversible hydrogen adsorption results a steady-state θ_H on the nanoparticles, which are in the form of PdH. The rate-determining addition of surface hydrogen to CO_2 forms adsorbed CO_2H, which is subsequently rapidly reduced by one e^- to form HCO_2^-. (Alternatively, CO_2H could be rapidly hydrogenated and then deprotonated to form HCO_2^-.) On Pd, hydrogen adsorption follows a Temkin isotherm,[40] meaning that the adsorption energy is linearly dependent on θ_H in the range of intermediate coverage. With Temkin adsorption, the mechanism in Scheme 1 predicts the rate law in eq 5.

$$j = k_0[CO_2]\theta_H\exp(\beta g\theta_H) \quad (5)$$

where k_0 is a potential-independent constant, β is the symmetry factor and g is the dimensionless surface heterogeneity factor.[41,42] The term $\exp(\beta g\theta_H)$ accounts for the dependence of the activation barrier on θ_H for a reaction step that consumes surface hydrogen. The Temkin isotherm is given by eq 6, where E is the potential with respect to RHE and K_0 is the adsorption constant.[41,42]

$$\exp(g\theta_H) = K_0\exp(-EF/RT) \quad (6)$$

Substituting for $\exp(g\theta_H)$ and neglecting the pre-exponential θ_H, eq 5 is simplified to eq 7:

$$j = k_0K_0{}^{\beta}[CO_2]\exp(-\beta EF/RT) \quad (7)$$

which corresponds to eq 4 with $k = k_0K_0{}^{\beta}$ and $\alpha = \beta$. If β = 0.5, as is often assumed, a Tafel slope of 118 mV dec^{-1} would be obtained. The observed 150 mV dec^{-1} Tafel slope may indicate that β deviates from 0.5 for this reaction. At potentials <−0.1 V, the Tafel slope increases substantially (Figure 3a). This change likely indicates that θ_H is saturated, in which case eq 6 no longer holds. In addition, mass transport limitations in the cell and CO poisoning may also be contributing to the apparent electrokinetics at this point.

The data in Figure 3c,d also indicate that, at constant potential vs RHE, $j_{formate}$ increases by approximately a factor of 2−3 per pH unit. This effect could arise from a pH dependence of the hydrogen adsorption thermodynamics. To maintain the same potential vs RHE at different pH values, the potential with respect to a pH independent reference such as Ag/AgCl must be adjusted by −59 mV per pH unit. This added potential

DOI: 10.1021/ja511890h
J. Am. Chem. Soc. 2015, 137, 4701−4708

could increase θ_H by increasing the adsorption constant K_0, leading to the observed rate increase.

We note that the rate expression in eq 4 is also consistent with the canonical mechanism for CO_2 reduction in which the reaction is rate-limited by an initial electron transfer to CO_2. While it cannot be ruled out based on the kinetics, this mechanism is very unlikely given the extremely low overpotentials required and the ability of Pd to chemically hydrogenate CO_2 as described above. Reduction of CO_2 by electrohydrogenation suggests that manipulation of the hydrogen adsorption energy on Pd may be a fruitful avenue for further improving the catalytic rate.

Pd/C has a relatively high rate of HCO_2^- synthesis in freshly prepared N_2-saturated electrolytes with high $[HCO_3^-]$ because there is an appreciable $[CO_2]$ from the equilibrium with HCO_3^-. However, sustaining this activity over a long electrolysis in N_2-saturated solution would be problematic because accumulation of CO_3^{2-} would increase the pH and decrease $[CO_2]$. Using a combination of CO_2 saturation and high $[HCO_3^-]$ is optimal for HCO_2^- synthesis with Pd/C because it maximizes pH while maintaining a high $[CO_2]$.

Our results illuminate the chemical challenges that must be addressed to make the use of Pd practical for HCO_2^- synthesis. Foremost is the poisoning by CO that forms as a minor CO_2 reduction product. CO inhibits all electroreduction activity at the potential range studied here. A promising strategy to solve this problem is to alloy Pd with another metal and thereby weaken the CO binding affinity.[43−47] Alloying may also reduce the rate of CO formation. Alternatively, Pd catalysts could be reactivated in situ by brief oxidative treatment. The other major challenge is to reduce nanoparticle sintering to preserve high mass activity over long electrolyses. This will likely require strengthening the nanoparticle-support interaction by changing the surface chemistry of carbon or using an alternative support such as a conductive metal oxide.

The inhibition of electrocatalytic activity by CO at low overpotential on Pd contrasts with the steady-state CO_2 reduction to CO at high overpotential.[15−18] At high overpotential, Pd has a high surface coverage of CO and steady-state CO_2 reduction to CO under these conditions may occur on a low density of sites that have weaker affinity for CO. Transition from HCO_2^- production to CO production occurs when the surface is covered by CO and the overpotential is sufficiently high to sustain CO_2 reduction at these sites.

The maximum geometric current density for CO_2 reduction in the electrochemical cells used here is limited to ∼10 mA cm^{-2}. Significantly higher geometric current densities require thick catalyst layers in electrochemical cells that have a gas diffusion electrode or a flowing electrolyte. Numerous reports have described cells engineered for high current density CO_2 reduction to HCO_2^- using non-Pd cathodes.[9,48−53] State-of-the-art flow cell electrolyzers with cathodes comprised of 3 mm−thick granular Sn layers were reported to have 120 mA cm^{-2} with 80% FE for HCO_2^- at a cell voltage of 3.4 V and a high flow rate of pure CO_2 through the electrolyte.[50] Given their high mass activity, we anticipate that dispersing Pd (alloy) nanoparticles on thicker, porous supports and using a flowing electrolyte will enable synthetically useful geometric current densities at much lower cell voltages while maintaining high Pd mass activities.

Approximately 600 000 tons of HCO_2H and HCO_2^- salts are produced annually. While this scale is a relatively small carbon footprint, replacing even a portion of the current synthesis with a CO_2 conversion process would provide a foundation for other CO_2 recycling efforts. Moreover, bioengineering[54] or new synthetic methodologies could make HCO_2H/HCO_2^- a feedstock for the synthesis of multicarbon products, increasing the demand for this compound. Energetically efficient reduction of CO_2 to HCO_2^- is essential for a scalable synthesis. We have shown that Pd is a promising candidate for an electrochemical process that meets this requirement.

CONCLUSION

In summary, Pd/C catalyzes the reduction of CO_2 into HCO_2^- with high mass activity and near quantitative Faraday efficiency at low overpotential in both CO_2- and N_2-saturated HCO_3^- solutions. The electrokinetic data support an electrohydrogenation mechanism whereby CO_2 is reduced by an electrochemically generated Pd hydride surface. This mechanism avoids the high-overpotential electron transfer steps typically required for electrochemical CO_2 reduction. Pd nanoparticles deactivate at a potential-dependent rate due to the formation of CO in a minor pathway. The CO poisons HCO_2^- synthesis at low overpotential, but CO can be removed by brief air exposure to restore activity.

ASSOCIATED CONTENT

Supporting Information

Experimental procedures and additional data. This material is available free of charge via the Internet at http://pubs.acs.org.

AUTHOR INFORMATION

Corresponding Author

*mkanan@stanford.edu

Notes

The authors declare no competing financial interest.

ACKNOWLEDGMENTS

We thank Stanford University, the Hellman Foundation, and the NSF (CHE-1266401) for support of this work. X.M. gratefully acknowledges a Stanford Office of Technology Licensing Fellowship.

REFERENCES

(1) Quadrelli, E. A.; Centi, G.; Duplan, J. L.; Perathoner, S. *ChemSusChem* **2011**, *4*, 1194−1215.
(2) Appel, A. M.; Bercaw, J. E.; Bocarsly, A. B.; Dobbek, H.; DuBois, D. L.; Dupuis, M.; Ferry, J. G.; Fujita, E.; Hille, R.; Kenis, P. J. A.; Kerfeld, C. A.; Morris, R. H.; Peden, C. H. F.; Portis, A. R.; Ragsdale, S. W.; Rauchfuss, T. B.; Reek, J. N. H.; Seefeldt, L. C.; Thauer, R. K.; Waldrop, G. L. *Chem. Rev.* **2013**, *113*, 6621−6658.
(3) Aresta, M.; Dibenedetto, A.; Angelini, A. *Chem. Rev.* **2014**, *114*, 1709−1742.
(4) Hull, J. F.; Himeda, Y.; Wang, W. H.; Hashiguchi, B.; Periana, R.; Szalda, D. J.; Muckerman, J. T.; Fujita, E. *Nat. Chem.* **2012**, *4*, 383−388.
(5) Ziebart, C.; Federsel, C.; Anbarasan, P.; Jackstell, R.; Baumann, W.; Spannenberg, A.; Beller, M. *J. Am. Chem. Soc.* **2012**, *134*, 20701−20704.
(6) Wang, W. H.; Hull, J. F.; Muckerman, J. T.; Fujita, E.; Himeda, Y. *Energy Environ. Sci.* **2012**, *5*, 7923−7926.
(7) Behr, A.; Nowakowski, K. In *CO_2 Chemistry*; Aresta, M., Eldik, R. V., Eds.; Elsevier: San Diego, 2014.
(8) Jeletic, M. S.; Mock, M. T.; Appel, A. M.; Linehan, J. C. *J. Am. Chem. Soc.* **2013**, *135*, 11533−11536.
(9) Agarwal, A. S.; Zhai, Y. M.; Hill, D.; Sridhar, N. *ChemSusChem* **2011**, *4*, 1301−1310.

DOI: 10.1021/ja511890h
J. Am. Chem. Soc. 2015, 137, 4701−4708

(10) Lu, X.; Leung, D. Y. C.; Wang, H.; Leung, M. K. H.; Xuan, J. *ChemElectroChem* **2014**, *1*, 836−849.
(11) Costentin, C.; Robert, M.; Saveant, J. M. *Chem. Soc. Rev.* **2013**, *42*, 2423−2436.
(12) Qiao, J.; Liu, Y.; Hong, F.; Zhang, J. *Chem. Soc. Rev.* **2014**, *43*, 631−675.
(13) Stalder, C. J.; Chao, S.; Wrighton, M. S. *J. Am. Chem. Soc.* **1984**, *106*, 3673−3675.
(14) Hori, Y. In *Modern Aspects of Electrochemistry*; Vayenas, C. G., White, R. E., Gamboa-Aldeco, M. E., Eds.; Sringer: New York, 2008; Vol. *42*, pp 89−189.
(15) Azuma, M.; Hashimoto, K.; Hiramoto, M.; Watanabe, M.; Sakata, T. *J. Electrochem. Soc.* **1990**, *137*, 1772−1778.
(16) Noda, H.; Ikeda, S.; Oda, Y.; Imai, K.; Maeda, M.; Ito, K. *Bull. Chem. Soc. Jpn.* **1990**, *63*, 2459−2462.
(17) Ohkawa, K.; Hashimoto, K.; Fujishima, A.; Noguchi, Y.; Nakayama, S. *J. Electroanal. Chem.* **1993**, *345*, 445−456.
(18) Hori, Y.; Wakebe, H.; Tsukamoto, T.; Koga, O. *Electrochim. Acta* **1994**, *39*, 1833−1839.
(19) Zhang, S.; Kang, P.; Meyer, T. J. *J. Am. Chem. Soc.* **2014**, *136*, 1734−1737.
(20) Chen, Y. H.; Kanan, M. W. *J. Am. Chem. Soc.* **2012**, *134*, 1986−1989.
(21) Kang, P.; Zhang, S.; Meyer, T. J.; Brookhart, M. *Angew. Chem., Int. Ed.* **2014**, 53 Early View.
(22) Kang, P.; Meyer, T. J.; Brookhart, M. *Chem. Sci.* **2013**, *4*, 3497−3502.
(23) Zhang, S.; Kang, P.; Ubnoske, S.; Brennaman, M. K.; Song, N.; House, R. L.; Glass, J. T.; Meyer, T. J. *J. Am. Chem. Soc.* **2014**, *136*, 7845−7848.
(24) Podlovchenko, B. I.; Kolyadko, E. A.; Lu, S. G. *J. Electroanal. Chem.* **1994**, *373*, 185−187.
(25) Kortlever, R.; Balemans, C.; Kwon, Y.; Koper, M. T. M. *Catal. Today* **2015**, *244*, 58−62.
(26) Furuya, N.; Yamazaki, T.; Shibata, M. *J. Electroanal. Chem.* **1997**, *431*, 39−41.
(27) Roy, R. N.; Gibbons, J. J.; Baker, G.; Simonson, J. M.; Pitzer, K. S. *J. Chem. Thermodyn.* **1984**, *16*, 303−315.
(28) Fang, L. L.; Tao, Q. A.; Li, M. F.; Liao, L. W.; Chen, D.; Chen, Y. X. *Chin. J. Chem. Phys.* **2010**, *23*, 543−548.
(29) Wang, J. Y.; Zhang, H. X.; Jiang, K.; Cai, W. B. *J. Am. Chem. Soc.* **2011**, *133*, 14876−14879.
(30) Obradovic, M. D.; Gojkovic, S. L. *Electrochim. Acta* **2013**, *88*, 384−389.
(31) Zhang, H. X.; Wang, S. H.; Jiang, K.; Andre, T.; Cai, W. B. *J. Power Sources* **2012**, *199*, 165−169.
(32) Zhou, W. J.; Lee, J. Y. *Electrochem. Commun.* **2007**, *9*, 1725−1729.
(33) Peter, M.; Flores Camacho, J. M.; Adamovski, S.; Ono, L. K.; Dostert, K. H.; O'Brien, C. P.; Roldan Cuenya, B.; Schauermann, S.; Freund, H. J. *Angew. Chem.* **2013**, *52*, 5175−5179.
(34) Peter, M.; Adamovsky, S.; Flores Camacho, J. M.; Schauermann, S. *Faraday Discuss.* **2013**, *162*, 341.
(35) Stuve, E. M.; Madix, R. J.; Brundle, C. R. *Surf. Sci.* **1984**, *146*, 155−178.
(36) Reda, T.; Plugge, C. M.; Abram, N. J.; Hirst, J. *Proc. Natl. Acad. Sci. U. S. A.* **2008**, *105*, 10654−10658.
(37) Klibanov, A. M.; Alberti, B. N.; Zale, S. E. *Biotechnol. Bioeng.* **1982**, *24*, 35−36.
(38) Stalder, C. J.; Chao, S.; Summers, D. P.; Wrighton, M. S. *J. Am. Chem. Soc.* **1983**, *105*, 6318−6320.
(39) Gabrielli, C.; Grand, P. P.; Lasia, A.; Perrot, H. *J. Electrochem. Soc.* **2004**, *151*, A1937−A1942.
(40) Breiter, M. W. *J. Electroanal. Chem.* **1977**, *81*, 275−284.
(41) Gileadi, E. *Electrode Kinetics for Chemists, Engineers, and Materials Scientists*; Wiley-VCH: New York, 1993.
(42) Saraby-Reintjes, A. *J. Chem. Soc., Faraday Trans. 1* **1987**, *83*, 271−279.
(43) Jiang, K.; Xu, K.; Zou, S. Z.; Cai, W. B. *J. Am. Chem. Soc.* **2014**, *136*, 4861−4864.
(44) Sakong, S.; Mosch, C.; Gross, A. *Phys. Chem. Chem. Phys.* **2007**, *9*, 2216−2225.
(45) Jeroro, E.; Lebarbler, V.; Datye, A.; Wang, Y.; Vohs, J. M. *Surf. Sci.* **2007**, *601*, 5546−5554.
(46) Ma, Y.; Bansmann, J.; Diemant, T.; Behm, R. J. *Surf. Sci.* **2009**, *603*, 1046−1054.
(47) Ma, Y. S.; Diemant, T.; Bansmann, J.; Behm, R. J. *Phys. Chem. Chem. Phys.* **2011**, *13*, 10741−10754.
(48) Li, H.; Oloman, C. *J. Appl. Electrochem.* **2005**, *35*, 955−965.
(49) Li, H.; Oloman, C. *J. Appl. Electrochem.* **2006**, *36*, 1105−1115.
(50) Li, H.; Oloman, C. *J. Appl. Electrochem.* **2007**, *37*, 1107−1117.
(51) Prakash, G. K. S.; Viva, F. A.; Olah, G. A. *J. Power Sources* **2013**, *223*, 68−73.
(52) Del Castillo, A.; Alvarez-Guerra, M.; Irabien, A. *AIChE J.* **2014**, *60*, 3557−3564.
(53) Narayanan, S. R.; Haines, B.; Soler, J.; Valdez, T. I. *J. Electrochem. Soc.* **2011**, *158*, A167−A173.
(54) Fast, A. G.; Papoutsakis, E. T. *Curr. Opin. Chem. Eng.* **2012**, *1*, 380−395.

DOI: 10.1021/ja511890h
J. Am. Chem. Soc. 2015, 137, 4701−4708